

# Simulation of Radar Cross Section (RCS) of Spherical Objects

Iroegbu Chibuisi,

Department of Electrical/Electronics Engineering, Michael Okpara University of Agriculture,  
Umudike, Abia State, Nigeria.

**Abstract:** This research is on Computer Simulation of Radar Cross Section (RCS) of spherical object. Radar Cross Section (RCS) is one of the key parameters in the detection of targets. It is used to describe the amount of scattered power from a target towards the radar. It has been observed that the radar designers use RCS of spherical shaped objects as a reference point in determining the RCS of other objects. This is because the RCS of a sphere tends to be constant. In this research, RCS of a sphere were simulated in the three regions of the sphere using matlab simulation tool to determine the exact region of the sphere where the RCS is constant. Observations during simulation of the data in the Rayleigh region showed that in this region, RCS dB ( $m^2$ ) varied approximately in amplitude and phase. For the MIE or resonance region, it was seen that there were a significant phase variation of the graph, which meant that the target was significant and all parts contributed to the scattering in this region. Furthermore, it was observed that the backscattered RCS for a perfectly conducting sphere was constant in the optical region.

**Keywords:** Radar Cross Section (RCS), Matlab, Spherical Object, Rayleigh Region, Resonance Region, Optical Region

## I. INTRODUCTION

Radar is an electromagnetic system for detecting, locating and sometimes for recognition of target objects, which operates by transmitting electromagnetic signals, receiving echoes from target objects within its volume of coverage, and extracting location and other information from the echo [1]. Once reflected signals are received, the range to a target can be calculated by evaluating

the interval of the radar signal's travel; the half time of total interval gives the distance of the target while the radar signal propagates from the transmitter and returns to the receiver after reflection from the target. It can be used in Civilian applications (Airport surveillance, Marine navigation, Weather Radar, Altimetry, Aircraft Landing, Security alarms, Speed measurement and Geographic mapping), Military applications (Air and marine navigation, Detection and tracking of aircraft, missiles, and super crafts, Fire control for missiles and artillery, and Reconnaissance), and Scientific application (Astronomy, Mapping and imaging, Precision distance measurement and Remote sensing of the environment) etc.

The ability of the radar to detect and analyze the shape, range, effective capture area and size of an object is the chief attributes of the Radar Cross Section (RCS) [2]. Therefore, in the design phase of the Radar system, it is often desirable to employ a computer to predict what the RCS will look like before deploying the actual system.

RCS of an object is the cross-sectional area that would produce reflection of the electromagnetic wave which is sent and observed in the Radar that functions as the source. It has been observed that the radar designers use RCS of spherical shaped objects as a reference point in determining the RCS of other objects. This is because the RCS of a sphere tends to be constant [3]. In this research, RCS of a sphere were simulated in the three regions of the sphere using matlab simulation tool to determine the exact region of the sphere where the RCS is constant. The remaining sections of the research are as follows: Section two dealt with the radar cross section, scattering regions and radar cross section prediction techniques, section three is on the materials and method used for the

research, section four presents the results and discussion, while section five concludes the work.

## II. RADAR CROSS SECTION

A target is detected by the radar only when the radar's receiver gets adequate energy back from the target, furthermore, this energy must be above the electronic noise or signal to noise threshold to be detected. There are many variables in the transmission scattering- reflection sequence which determine the maximum detection range. These are transmitter effective outgoing energy, beam width, RCS of the target, total energy back from the target, antenna aperture (or size) and the receiver's processing capability. Among these variables, RCS is the main concern of this study. Radar cross section is the size of a target as seen by the radar. In more scientific words, RCS is a measure of the power that is returned or scattered in a given direction, normalized with respect to power density of the incident field. The normalization is made to remove the effect of the range, and so the signature is not dependent on the distance between the target and the receiver. Assume the power density of a wave incident on a target located at range R away from the radar is  $E_0$ . The amount of reflected power from the target is

$$E_s = \sigma E_0 \dots \dots \dots (1)$$

$\sigma$  denotes the target cross section.  $E_0$  is defined as the power density of the scattered waves at the receiving antenna. It follows that

$$E_0 = E_s / (4\pi R^2) \dots \dots \dots (2)$$

Equating equations (1) and (2) yields

$$\sigma = \lim_{R \rightarrow \infty} 4\pi R^2 \frac{|E_s|^2}{|E_0|^2} \text{ or } \dots \dots \dots (3)$$

$$\sigma = \lim_{R \rightarrow \infty} \frac{4\pi R^2 \times \text{power density in scattered field}}{\text{power density of incident planewave}}$$

Therefore, the RCS can also be defined as  $4\pi$  times the ratio of the power per unit solid angle scattered in a specified direction to the power per unit area in a plane wave incident on the scatterer from a specified direction.

where  $\sigma$  is the RCS of the target, R the range between radar and target,  $E_s$  the scattered electric field, and  $E_0$  the incident electric field.

The unit of cross section is usually given in square meters. Due to the large variation in RCS pattern from one aspect angle to another, it is convenient to display the RCS in logarithmic form. The unit commonly used is decibel over a square meter or dBsm i.e.

$$\text{RCS (dBsm)} = 10 \log_{10} \sigma \dots \dots \dots (3)$$

RCS of a target will have a wide variation, if the illuminating electromagnetic wave has got a wide range of frequencies. The variation of RCs with frequency is classified into three regions, depending on the size of the object. In the first region, the target dimensions are small compared to wavelength. This is called the Rayleigh region, and is proportional to the fourth power of frequency. In the second region, the target dimensions are approximately equal to the wavelength. This region is known as the resonance region. In the third region, the object dimensions are much larger than the wavelength. This region is called the optical region.

The knowledge of RCS characteristics of some simple targets is very important in RCS measurement and analysis of complex targets. Complex targets such as missiles, ships, aircrafts etc. can be described as collections of relatively simple shapes like spheres, flat plates, cylinders, cones and corner reflectors. In measuring the RCS of complicated objects, the measurements are often calibrated by comparing the echo levels of the test objects with those of the calibration target. As the echo strength of the calibration target must be known with high degree of accuracy, the calibration target is always a simple one.

The factors which affect the RCS are:

- a. Material with which the target is made.
- b. Absolute size of the target.
- c. Relative size of the target (in relation to the wavelength of the illuminating Radar).
- d. The incident angle (angle at which the Radar beam hits a particular portion of the target which depends upon shape of target and its orientation to the Radar).

- e. Reflected angle (angle at which the reflected beam leaves the part of the target hit, it depends upon incident angle).
- f. The polarization of transmitted and the received radiation in respect to the orientation of the target.
- g. Position of radar antenna relative to target
- h. Frequency of the electromagnetic energy

### A. Scattering Regions

The Radar Cross Section depends on the frequency of the incident wave. There are three frequency regions in which the RCS of a target is distinctly different. The regions are defined based on the size of the target in terms of the incident wavelength. For a smooth target of length  $L$ , the definitions of the three frequency regimes follow.

1. Low frequency region or Rayleigh region ( $\frac{2\pi}{\lambda} L \ll 1$ )

At these frequencies, the phase variation of the incident plane wave across the extent of the target is small. Thus, the induced current on the body of the target is approximately constant in amplitude and phase. The particular shape of the body is not important. Generally,  $\sigma$  versus  $\frac{2\pi}{\lambda} L$  is smooth and varies as  $1/\lambda^2$ .

2. Resonance region or mie region ( $\frac{2\pi}{\lambda} L \approx 1$ )

For these frequencies, the phase variation of the current across the body of the target is significant and all parts contribute to the scattering. Generally,  $\sigma$  versus  $\frac{2\pi}{\lambda} L$  and will oscillate.

3. High frequency region or optical region ( $\frac{2\pi}{\lambda} L \gg 1$ )

For these frequencies, there are many cycles in the phase variation of the current across the target body and, consequently, the scattered field will be very angle-dependent. In this region,  $\sigma$  versus  $\frac{2\pi}{\lambda} L$  is smooth and may be independent of  $\lambda$ .

The backscattered RCS for a perfectly conducting sphere is constant in the optical region. For this reason, radar designers typically use spheres of known cross sections to experimentally calibrate radar systems.

Figure 1 depicts the Radar Cross Section of a sphere with radius  $a$ , where  $\beta$  is defined as  $\beta = 2\pi/\lambda$ . The three scattering regions are clearly illustrated. When  $\beta a < 0.5$ , the curve in the Rayleigh region is almost linear. However, above 0.5, in the resonance region, the RCS oscillates. The oscillations die out as  $\beta a$  takes higher values. Eventually, for  $\beta a > 10$ , the value of the RCS is essentially constant and equal to  $\pi a^2$ .

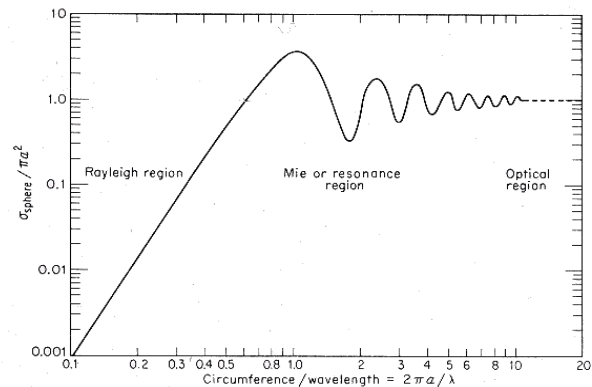


Figure 1: Radar cross section of a sphere [3].

### B. Radar Cross Section Prediction Techniques

Some of the most common numerical RCS prediction methods for any arbitrary dimensional target are the Method of Moments, the Finite Difference Method, Microwave Optics and Physical Optics. For each method, its advantages and limitations will be discussed.

#### 1. Method of moments

The most common technique used to solve an integral equation is the Method of Moments (MM) [3]. In the RCS prediction case, integral equations are derived from Maxwell's equations and the boundary conditions, with the unknown quantity being an electric or magnetic current (either volume or surface). The Method of Moments reduces the integral equations to a set of simultaneous linear equations that can be solved using standard matrix algebra. Most Method of Moments formulations require a discretization (segmentation) of the target body and, therefore, are compatible with finite element methods used in structural engineering. In fact, the two are frequently used in tandem during the design of a platform.

Another advantage of the Method of Moments is that it provides a rigorous solution to the RCS prediction problem, yielding very accurate results. However, this method tends to produce large matrices, resulting in high computational requirements and increased run time. In addition, since current computer capabilities allow the modeling of targets on the order of 10 to 20 wavelengths, the method is not practical for large targets at high frequencies due to computer limitations.

## 2. Finite difference methods

Finite Difference methods are used to approximate the differential operators in Maxwell's equations in either the time or frequency domain. Similar to the Method of Moments, the target must be discretized [4]. Maxwell's equations and the boundary conditions are enforced on the surface of the target and at the boundaries of the discretization cells. In the time domain, this method is used extensively in computing transient responses of targets to various waveforms. Since the solution is stepped in time throughout the scattering body, the finite difference method does not require large matrices as does the Method of Moments. Frequency domain data is obtained by Fourier-transforming the time data.

This method also provides a rigorous solution to the RCS prediction problem.

However, since it calculates the fields in a computational grid around the target, the calculation of the RCS of a target with a characteristic dimension of several orders of magnitude of the wavelength would entail considerable amount of time to execute.

## 3. Microwave optics

Ray tracing methods that can be used to analyze electrically large targets of arbitrary shape are referred to as Microwave Optics. This term actually refers to a collection of ray tracing techniques that can be used individually or in concert. The two most used are the Geometrical Optics (GO) method and the Geometrical Theory of Diffraction (GTD) method. The rules for ray tracing in a simple medium (i.e., linear, homogenous and isotropic) are similar to

reflection and refraction in optics. In addition, this method takes into account diffracted rays, which originate from the scattering of the incident wave at edges, corners and vertices. The formulae are derived on the basis of infinite frequency, which implies an electrically large target. The major disadvantage of this method is the bookkeeping required when tracking a large number of reflections and diffractions for complex targets.

## 4. Physical optics

The Physical Optics (PO) method estimates the surface current induced on an arbitrary body by the incident radiation. On the portions of the body that are directly illuminated by the incident field, the induced current is simply proportional to the incident magnetic field intensity. On the shadowed portion of the target, the current is set to zero. The current is then used in the radiation integrals to compute the scattered field far from the target. This method is a high frequency approximation that provides the best results for electrically large targets as well as in the specular direction [5].

Physical optics is derived from Maxwell's equations [6]. The starting point is Stratton-Chu integral equations, which are obtained by transforming Maxwell's equations into a pair of integral equations.

$$E_s = \int \{ ikZ_0(n \times H)\Psi + (n \times E) \times \nabla\Psi + (n \cdot E)\nabla\Psi \} ds \dots\dots\dots(4)$$

$$H_s = \int \{ -ikY_0(n \times E)\Psi + (n \times H) \times \nabla\Psi + (n \cdot H)\nabla\Psi \} + ds \dots\dots\dots(5)$$

where  $E_s$  and  $H_s$  are the scattered electric and magnetic fields,  $E$  and  $H$  the total electric and magnetic field,  $k$  the radian frequency,  $Z_0$  and  $Y_0$  the permeability,  $n$  the unit surface normal erected to the surface patch  $dS$ .

Green's Function  $\Psi$  is

$$\Psi = \frac{e^{ikr}}{4\pi r} \dots\dots\dots(6)$$

where  $r$  is the distance from the surface patch  $dS$  to the radar. The theory is based on two approximations. The first is far-field approximation, which requires that the range be



large compared to any dimension of the object. The Green's function becomes

$$\nabla\Psi = ik\Psi_0s \dots\dots\dots(7)$$

$$\Psi = \frac{e^{-ikr} \times s \times e^{ikR_0}}{4\pi R_0} \dots\dots\dots(8)$$

where  $s$  is the position vector,  $r$  the unit vector, and  $R_0$  the distance from origin to radar.

The second approximation is tangent plane approximation.

If the surface is a good conductor, the total tangential electric field is virtually zero and the total tangential magnetic field is twice the amplitude of the incident tangential magnetic field. The tangent plane approximation results are

$$n \times E = 0 \dots\dots\dots(9)$$

$$n \times H = 2n \times H_i \text{ for illuminated surfaces } \dots\dots(10)$$

$$n \times H = 0 \text{ for shaded surfaces } \dots\dots\dots(11)$$

**C. Prediction Of RCS Through Computer Software**

Computer software is widely used to make calculations in all fields of engineering due to immense computational power and ease of graphical interfacing. Computer software based on low frequency methods or high frequency methods is available. Low frequency software is used for small objects to validate high frequency software and new techniques. High frequency software is used for RCS analysis of complex objects such as naval ships. The process consists of RCS prediction and evaluating design variations to reduce the RCS on naval ships in the same way as other military platforms [7][8]. Modern high frequency RCS software uses a combination of high frequency methods to determine the RCS of objects. The effectiveness of the software depends on the choice of methods used to account for different scattering mechanisms and computational time. However, computational time is a lesser concern with availability of high power computers and parallel processing.

In this research, we utilized the physical optics along with one or more methods to account for different scattering mechanisms. Then, the

radiation integrals are used to compute the scattered field.

**III. MATERIALS AND METHOD**

**A. Materials**

Radar designers and RCS engineers consider the perfectly conducting sphere to be the simplest target to examine. Due to symmetry, waves scattered from a perfectly conducting sphere are co-polarized (have the same polarization) with the incident waves. This means that the cross-polarized backscattered waves are practically zero. Most formulas presented are Physical Optics (PO) approximation for the backscattered RCS measured by far field radar in the direction  $(\theta, \phi)$ . The direction of antenna receiving backscattered waves is shown in Figure 2.

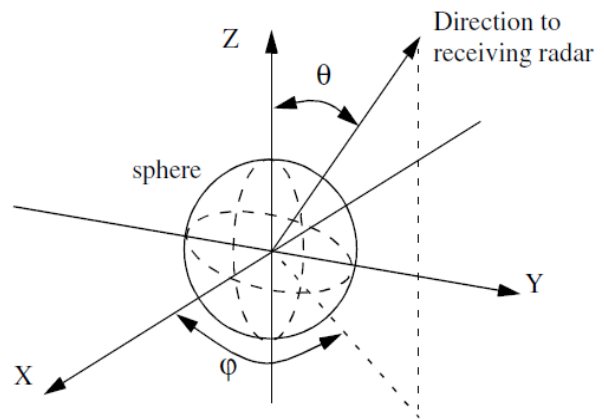


Figure 2: Scattered wave from sphere

The normalized exact backscattered RCS for a perfectly conducting sphere in a Mie series is given by:

$$\frac{\sigma}{\pi r^2} = \left(\frac{1}{kr}\right) \sum_n^\infty = 1(-1)^n(2n+1) \left[ \left( \frac{kr j_n(kr) - nj_n(kr)}{kr H_{n-1}(kr) - n H_n^1(kr)} \right) - \left( \frac{j_n(kr)}{H_n^1(kr)} \right) \right] \dots\dots\dots(12)$$

Here,  $r$  is radius of sphere,  $k = 2\pi/\lambda$ ,  $\lambda$  is wavelength  $j_n$  is spherical Bessel of the first kind of order  $n$ ,  $H_n^1$  is the Hankel function of order  $n$ , and is given by

$$H_n^1(kr) = j_n(kr) + jy_n(kr) \dots\dots\dots(13)$$

$y_n$  is the spherical Bessel function of the second kind of order  $n$ .

In this research, Plots of the normalized perfectly conducting sphere RCS with a radius( $r$ ) =15 cm as a function of its circumference in wavelength units are constructed.

### B. Methods

The flow chart in Figure 3 illustrates the sequence followed in computer simulation of Radar Cross Section (RCS) of a spherical object

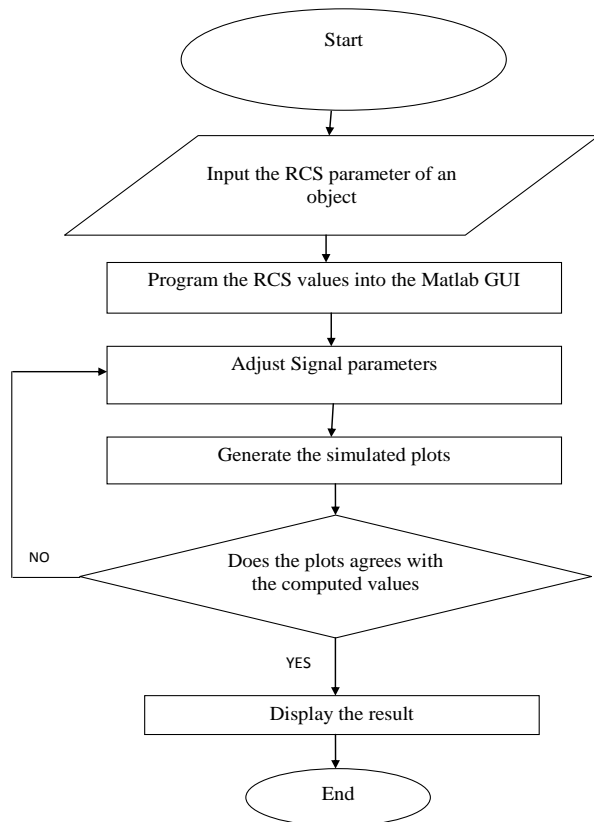


Figure 3: Design flow chart

## IV. RESULTS AND DISCUSSION

### A. Results

When a sphere is simulated in three regions, the first is the Rayleigh region, the second is the MIE or resonance region and the third is optical region. Observations during simulation of data resulted in measurement of  $r=15$  cm (radius).

RCS in dB ( $m^2$ ) in the Rayleigh region started at 0dB ( $m^2$ ) and ended at 1dB ( $m^2$ ) for the data. At circumference of 1( $m^2$ ), the RCS dB ( $m^2$ ) rises to 1.9 dB ( $m^2$ ). The positive overshoot at the Rayleigh region is seen to 0.9 i.e. (90%), while

the negative overshoot is seen to be 0.58 i.e. (58%).

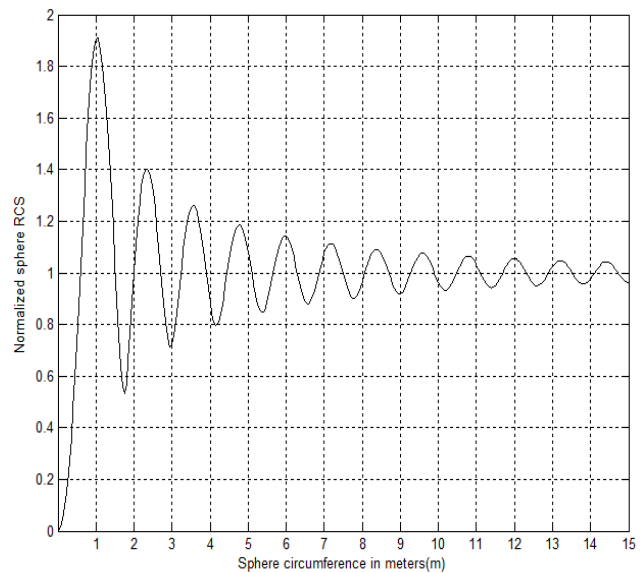


Figure 4: Cartesian plot for Rayleigh region

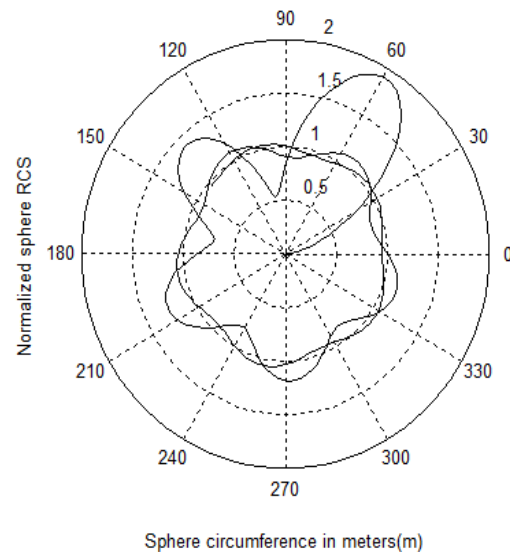


Figure 5: Polar plot for Rayleigh region

RCS in dB ( $m^2$ ) in the MIE or Resonance region started at -20dB ( $m^2$ ) and was seen to rise till 0.1dB ( $m^2$ ) for the data. At circumference of 1( $m^2$ ), the RCS dB ( $m^2$ ) rises till 4.0 dB ( $m^2$ ). The positive overshoot at the MIE region was seen to be 0.80 i.e. (80%), while the negative overshoot was seen to be -0.1 i.e. (-10%).

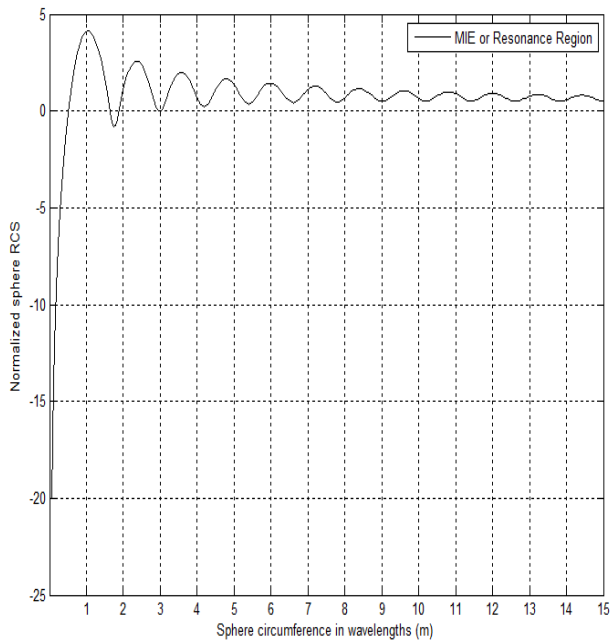


Figure 6: Cartesian plot for MIE or Resonance region

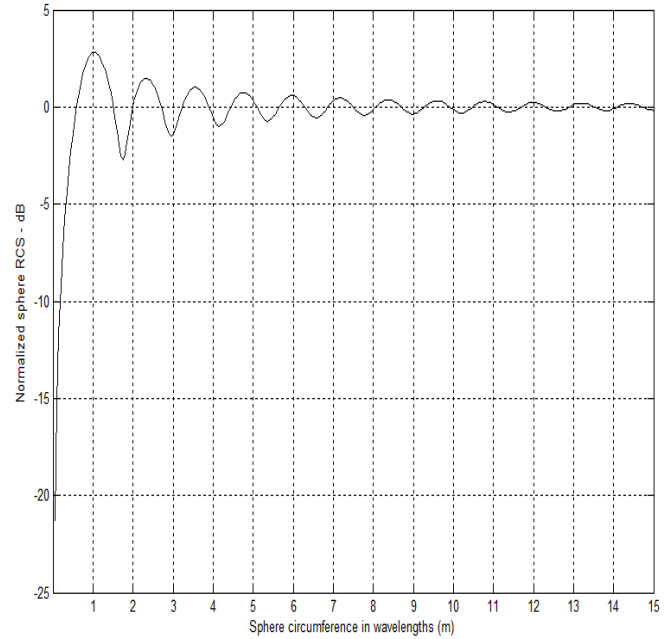


Figure 8: Cartesian plot for optical region

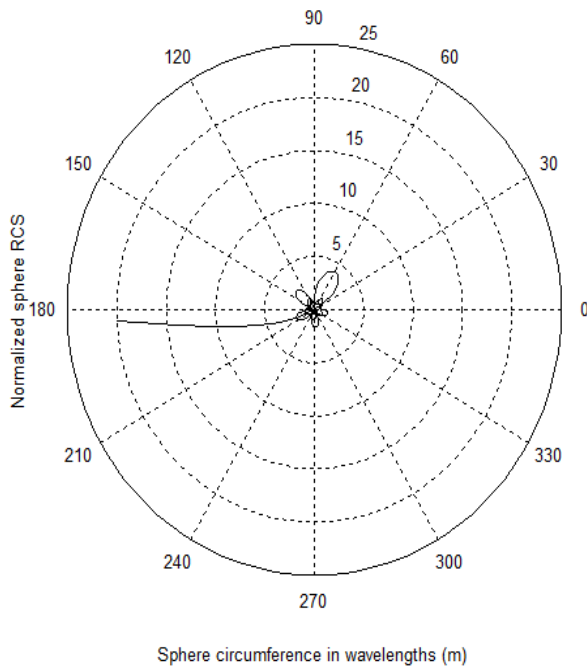


Figure 7: Polar plot for MIE or Resonance region

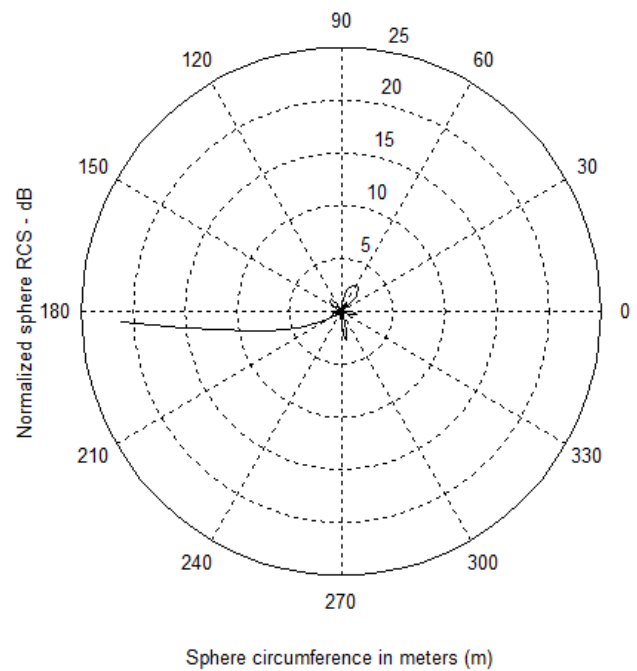


Figure 9: Polar plot for optical region

RCS in dB ( $m^2$ ) in the Optical region started at -22dB ( $m^2$ ) and was seen to rise till 0dB ( $m^2$ ) for the data. At circumference of 1( $m^2$ ), the RCS dB( $m^2$ ) rises till 2.5 dB( $m^2$ ). The positive overshoot at the Optical region is seen to be 0.50 i.e. (50%), while the negative overshoot was seen to be -0.5 i.e. (-50%).

Figure 10 shows the graph obtained in plotting the three regions of sphere together. While figure 11 also shows the graph obtained in plotting Rayleigh and MIE regions of the sphere together.

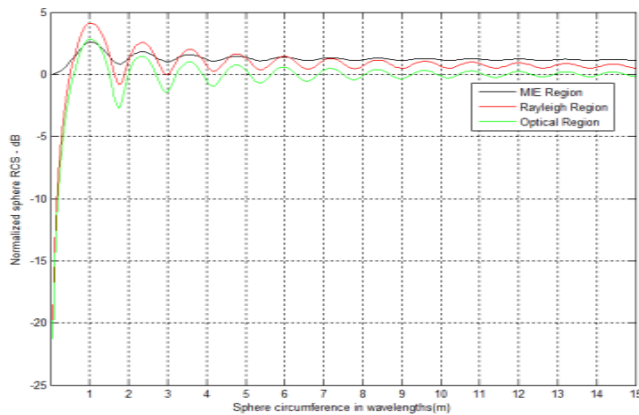


Figure 10: Comparison of the three regions of sphere

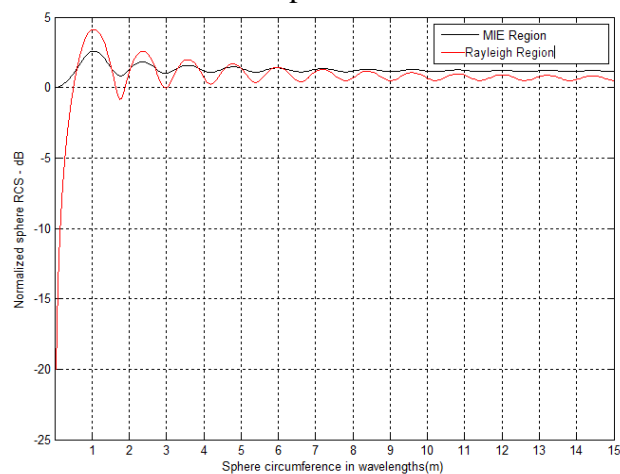


Figure 11: Comparison of Rayleigh and MIE regions of sphere

Figure 12 shows the graph obtained in plotting Rayleigh and Optical regions of the sphere together.

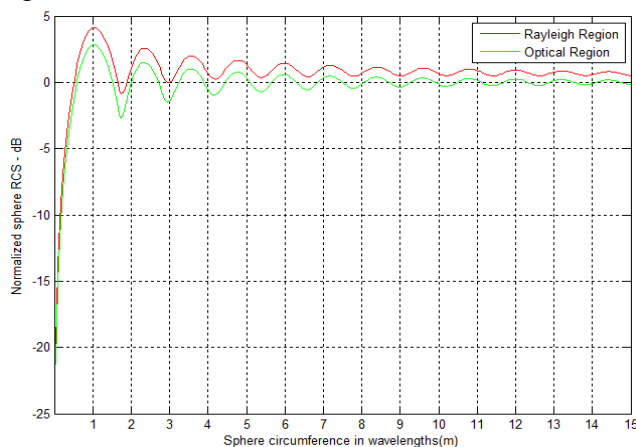


Figure 12: Comparison of Rayleigh and optical regions of sphere

From the three graphs above, we can summarize the results of the comparison of the three regions of sphere in Table 1.

Table 1: Results of the comparison of the three regions of sphere

Parameter	Rayleigh region	MIE region	Optical region
Overshoot	More (90%)	Less (80%)	Less (50%)
Rise time	More (80%)	Less (40%)	More (50%)
Transient	Present	Present	Present

The positive overshoot at the Rayleigh region is 0.9 i.e. (90%), while the negative overshoot is seen to be 0.58 i.e. (58%). The positive overshoot at the MIE region is 0.80 i.e. (80%), while the negative overshoot is seen to be -0.1 i.e. (-10%). Also the positive overshoot at the optical region is 0.50 i.e. (50%). The rise time in Rayleigh region is (80%), while that of MIE region is (40%) and optical region is (50%). Also, there are transient in all the three regions of sphere.

Therefore, the Radar designers should take note that there are more overshoot and rise time in Rayleigh region as compared to MIE and optical regions.

### B. Discussion

The sphere was simulated in three regions: the first was the Rayleigh region, the second the MIE or resonance region and the third was the optical region. Observations during simulation of the data in the Rayleigh region showed that in this region, RCS dB ( $m^2$ ) varied approximately in amplitude and phase. For the MIE or resonance region, it could be seen that there was a significant phase variation of the graph, which meant that in this region, the target was significant and all parts contributed to the scattering. The backscattered RCS for a perfectly conducting sphere was seen to be constant in the



optical region. For this reason, radar designers typically use spheres of known cross sections to experimentally calibrate radar systems. In terms of comparison, the result showed that there were more overshoot and rise time in the MIE Region compared to both the Rayleigh and Optical Regions. Also, transient was present in all the regions.

### CONCLUSION

The ability of the Radar system is to detect and analyze the shape, range, effective capture area and size of an object depends on the Radar Cross Section (RCS), thus, it became pertinent at the design phase of the Radar system to employ computer simulation software to predict what the RCS will look like before deploying the actual system.

Radar Cross-Section has been described as the ratio of radiated power density intercepted by a target to the power per unit solid angle backscattered to the receiving antenna by the target.

Its efficiency depends on shape, size, material composition, Frequency, Aspect angle, Surface area and other factors that vary widely between different types of target.

### References

- [1] Edde, B. (1993). Radar - Principles, Technology, Applications, Prentice-Hall, Englewood Cliffs, NJ.pp.78-89.
- [2] Knott E.F., Shaeffer J.F., Tuley M.T. (2004). Radar Cross Section, Second Edition. SciTech Publishing, Raleigh, NC, USA. Pp. 1-21 and 115-223.
- [3] Wong S. K., Riseborough E., Duff G., Chan K.K. (2006). Radar cross-section measurements of a full-scale aircraft duct/engine structure. IEEE Transactions on Antennas and Propagation, 54(8). Pp. 2436-2441.
- [4] Jansen C., Krumbholz N., Geise R., Enders A., Koch M. (2009). Scaled radar cross section measurements with terahertz-spectroscopy up to 800 GHz. European

Conference on Antennas and Propagation, Berlin, Germany. Pp. 3645-3648.

- [5] Skolnik M. I. (2008). Radar Handbook, Third Edition. McGraw-Hill Companies, New York, USA, Pp. 12-34.
- [6] Fang C. H., Zhao X. N., and Liu Q. (2008). An Improved Physical Optics Method for the Computation of Radar Cross Section of Electrically Large Objects. Asia-Pacific Symposium on Electromagnetic Compatibility & 19th International Zurich Symposium on Electromagnetic Compatibility, Singapore. Pp. 722-725.
- [7] Broek B. V. D., Bieker T., and Ewijk L. V. (2005). Comparison of Modelled to Measured High-Resolution ISAR Data. Netherlands Organization for Applied Scientific Research, Netherlands, TNO Report No. RTO-MP-SET-096.Pp.5-9.
- [8] Leong H. and Wilson H. (2006). An estimation and verification of vessel radar cross sections for high-frequency surface-wave radar. IEEE Antennas and Propagation Magazine, 48(2), pp. 11- 16.

### AUTHOR



Iroegbu Chibuisi is a PhD scholar in the department of Electrical and Electronics Engineering (Electronics and Communication option), Michael Okpara University of Agriculture, (MOUUA) Umudike, Abia State Nigeria. He holds a Bachelor degree (B.Eng) and Master's degree (M.Eng) in Electrical/Electronics Engineering (Electronics and Communication option). Iroegbu Chibuisi is also a member of International Association of Engineers. His research interests are in the fields of Radar systems, wireless sensor networks, Electronic and Communication Systems design and modeling, Security system design, Expert systems and Artificial Intelligence, Design of Microcontroller based systems, Channel coding, fading channels, interference management etc.